Current Biology 18, 44–50, January 8, 2008 ©2008 Elsevier Ltd All rights reserved DOI 10.1016/j.cub.2007.11.051

Report

Robust Neuronal Symmetry Breaking by Ras-Triggered Local Positive Feedback

Marc Fivaz,[1,2,*] Samuel Bandara,[1] Takanari Inoue,[1] and Tobias Meyer[1,*]
[1]Clark Center, Bio-X
Department of Chemical and Systems Biology
Stanford University
318 Campus Drive
Stanford, California 94305

Summary

Neuronal polarity is initiated by a symmetry-breaking event whereby one out of multiple minor neurites undergoes rapid outgrowth and becomes the axon [1]. Axon formation is regulated by phosphatidylinositol 3-kinase (PI3K)-related signaling elements [2–10] that drive local actin [11] and microtubule reorganization [3, 12], but the upstream signaling circuit that causes symmetry breaking and guarantees the formation of a single axon is not known. Here, we use live FRET imaging in hippocampal neurons and show that the activity of the small GTPase HRas, an upstream regulator of PI3K, markedly increases in the nascent axonal growth cone upon symmetry breaking. This local increase in HRas activity results from a positive feedback loop between HRas and PI3K, locally reinforced by vesicular transport of HRas to the axonal growth cone. Recruitment of HRas to the axonal growth cone is paralleled by a decrease in HRas concentration in the remaining neurites, suggesting that competition for a limited pool of HRas guarantees that only one axon forms. Mathematical modeling demonstrates that local positive feedback between HRas and PI3K, coupled to recruitment of a limited pool of HRas, generates robust symmetry breaking and formation of a single axon in the absence of extrinsic spatial cues.

Results and Discussion

HRas Regulates Axon Formation

Because the small GTPase Ras is a potent activator of PI3K [13], we investigated the role of Ras in symmetry breaking and axon formation. Overexpression of wild-type (WT) (CFP-HRas) or constitutively active (CFP-HRasQ61L) HRas in hippocampal neurons resulted in the formation of multiple axons (Figure 1A and Figure S1A available online), in agreement with a previous report [9]. Surprisingly, a constitutively active mutant of the closely related KRas isoform (CFP-KRasQ61L) failed to induce multiple axons (Figure 1A and Figure S1B), suggesting that HRas and KRas differentially regulate axon formation. To address the role of endogenous HRas in axon formation, we used an RNA-interference approach. Small interfering RNA (siRNA) knockdown of HRas increased the fraction of unpolarized neurons and reduced axon length in polarized neurons compared to a control siRNA after 72 hr in culture (Figured 1B and 1C and Figures S1C and S1D). A similar phenotype was observed with another HRas-targeting siRNA sequence (Figures S1C–S1F). Together, these results indicate that HRas regulates axon formation. Although KRas does not seem to regulate neuronal polarity, we found that a constitutively active mutant of NRas also induces multiple axons (Figure S1G), suggesting some redundancy in Ras isoform function. That different Ras isoforms contribute to axon formation is further supported by an earlier finding implicating RRas in neuronal polarity [14].

HRas Activity Is Spatially Confined to the Nascent Axonal Growth Cone

To examine the spatiotemporal dynamics of HRas signaling in developing neurons, we used a fluorescence resonance energy transfer (FRET)-based imaging assay that monitors the fraction of active guanosine-triphosphate (GTP)-bound HRas. We measured the relative FRET efficiency ($FRET_E$) between CFP-HRas (CFP: cyan fluorescent protein) and YFP-RBD (Ras Binding Domain of Raf-1) (YFP: yellow fluorescent protein), a reporter domain that selectively interacts with GTP-bound Ras [15]. $FRET_E$ is independent of CFP-HRas concentration and correlates linearly with the fraction of CFP-HRas bound to YFP-RBD [16, 17]. In unpolarized neurons, HRas activity was low and evenly distributed in the soma and neurites (Figure S2A). Upon symmetry breaking, however, HRas activity locally increased approximately 2-fold in the putative axonal growth cone (Figure 1D) and remained elevated in the axonal growth cone of polarized neurons (Figures 1E and 1F). The latter analysis was done in neurons with one axon only. These data suggest that local HRas activation has an early and sustained role in axon formation and outgrowth. We found no evidence for asymmetric KRas activity in developing neurons (Figures S2B and S2C).

HRas and PI3K Are Connected by a Positive Feedback Loop

The segregation of HRas activity in the emerging axon suggests that HRas might regulate local activation of PI3K and production of phosphatidylinositol-3,4,5-triphosphate (PIP3). We used the YFP-conjugated plextrin homology (PH) domain of Akt to monitor local PIP3 levels [18] and found that CFP-HRas and YFP-Akt-PH were coenriched in both nascent and more mature axons but did not colocalize in other regions of the cell (Figure S3C). This suggests that HRas locally activates PI3K and supports the notion that HRas regulates axon specification through local activation of PI3K and production of PIP3. Evidence that HRas is upstream of

*Correspondence: marc.fivaz@gms.edu.sg (M.F.), tobias1@stanford.edu (T.M.)
[2]Present address: Duke-National University of Singapore Graduate Medical School, Neurobehavioral Disorders Program, 2 Jalan Bukit Merah, Singapore 169547.

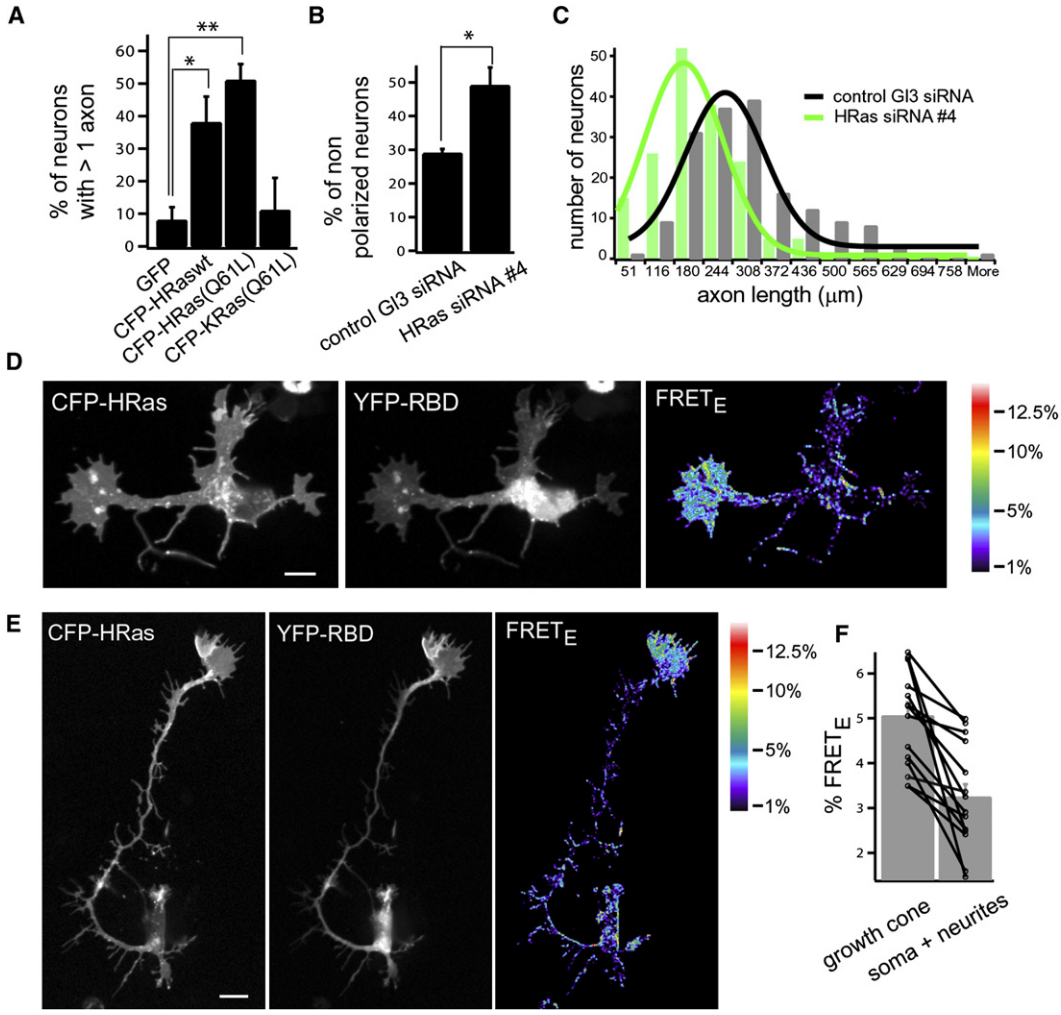

Figure 1. HRas Activity Is Locally Upregulated upon Symmetry Breaking and Axon Formation

(A) Hippocampal neurons (6 days in vitro, DIV) expressing CFP-HRas(WT) or CFP-HRas(Q61L) exhibited a marked multiple-axon phenotype compared to neurons expressing GFP or CFP-KRas(Q61L) (n > 50 for each condition; * indicates p = 0.002, and ** indicates p = 0.0003). Axons were identified with the axonal marker Tau-1. (See Figures S1A and S1B for image data).

(B and C) Silencing of endogenous HRas with synthetic siRNAs inhibited axon formation and reduced axon length (n > 150 for each condition). (B) shows the percent of unpolarized neurons after treatment with control or HRas siRNAs 72 hr after plating (* indicates p = 0.0009). (C) shows the distribution of axon length in neurons treated with GL3 (control) or HRas siRNAs. Median lengths were 250 ± 10 μm and 164 ± 7 μm, respectively ($p = 1.3 \times 10^{-11}$) (see also Figures S1C–S1F).

(D–F) FRET imaging of CFP-HRas- and YFP-RBD-expressing neurons revealed an increase in HRas activity in the putative axonal growth cone after symmetry breaking (D) and in axonal growth cones of polarized neurons (E). The relative FRET efficiency (FRET$_E$) is color encoded. (F) shows quantification of FRET$_E$ values for HRas in the axonal growth cone versus the soma and remaining neurites (n = 15, p = 0.0001).

Error bars represent the standard error of the mean.

PI3K in neurons came from the work of Yoshimura et al. [9], who showed that PI3K inhibition by LY294002 suppresses the multiple-axon phenotype observed upon HRas overexpression.

What controls local activation of HRas? We postulated that HRas is selectively activated in the future axonal growth cone by a positive feedback loop, whereby PI3K signals back to activate HRas. A similar feedback circuit has been proposed to operate at the leading edge of *Dictyostelium discoideum* cells during chemotaxis [19, 20]. To test this hypothesis, we asked whether the increase in HRas activity in the axonal growth cone requires that the downstream target PI3K is active. Strikingly, addition of the reversible PI3K inhibitor LY294002 led to a rapid decrease of HRas activity, which was restored upon LY294002 washout and stimulation of Ras by Brain Derived Neurotrophic Factor (BDNF) (Figures 2A and 2B; see Movie S1). The time constant of LY294002-induced HRas inactivation is about 1 min (Figures 2B and 2C). This argues that HRas activity is enhanced in the axonal growth cone by a rapid positive feedback loop between HRas and PI3K.

We then asked whether the feedback from PI3K to Ras is a general mechanism and investigated whether epidermal growth factor (EGF)-induced activation of Ras in fibroblasts is PI3K dependent. Addition of EGF leads to a robust and sustained Ras activation in Rat-2 fibroblasts, as measured by FRET (Figures S4A and S4B). After EGF-induced Ras activation, treatment with LY294002 resulted in a rapid decrease of Ras activity

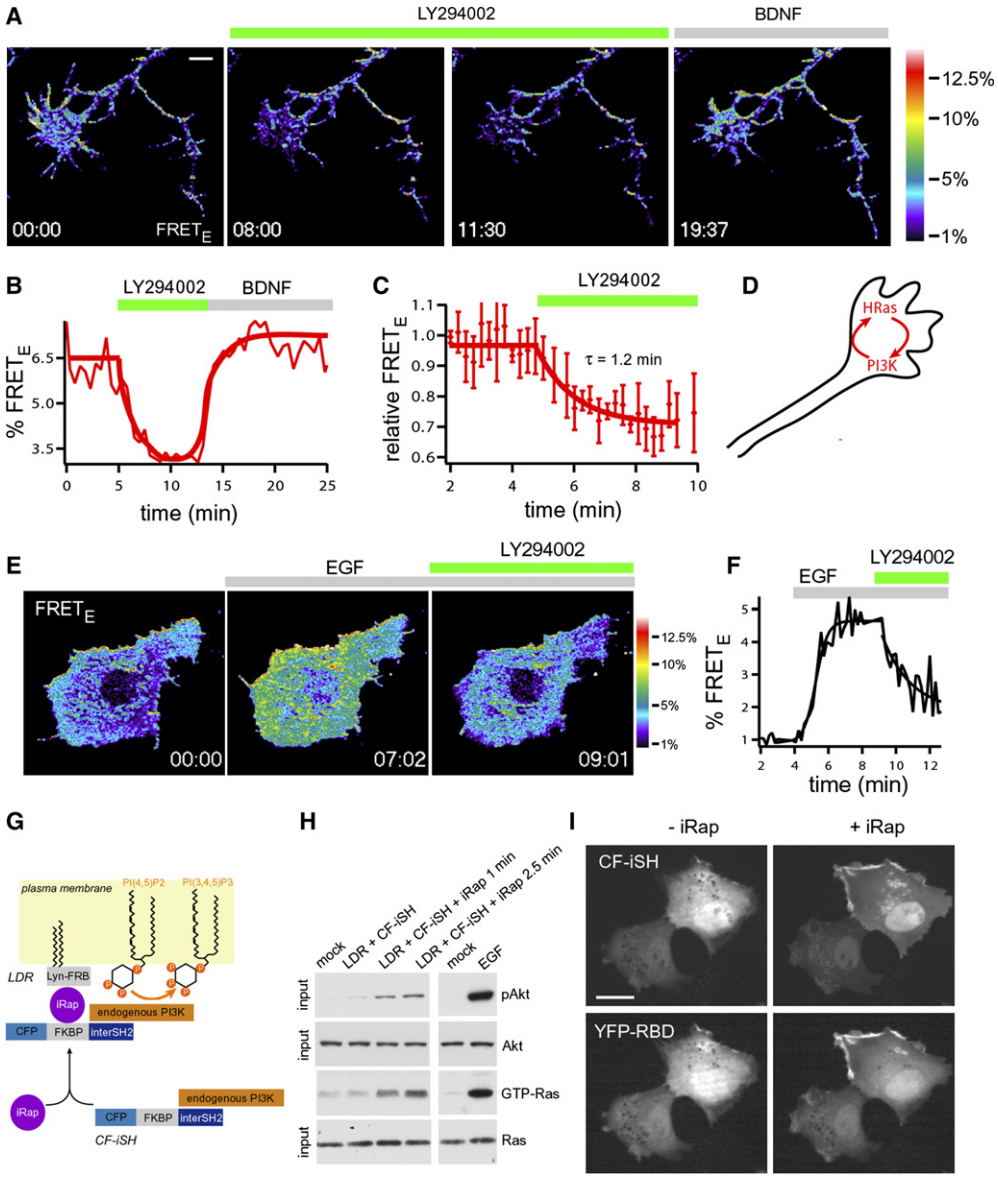

Figure 2. HRas and PI3K Are Connected by Positive Feedback

(A) FRET$_E$ time-lapse analysis shows a rapid decrease of the fraction of active GTP-bound HRas in the axonal growth cone of DIV 3 neurons upon addition of the PI3K inhibitor LY294002 (50 μM). HRas activity was restored upon LY294002 washout and brain-derived neurotrophic factor (BDNF) (50 ng/ml) stimulation (see Movie S1).

(B) Average FRET$_E$ value in the axonal growth cone shown in (A).

(C) Kinetics of LY294002-induced HRas inactivation in the axonal growth cone (n = 6). The decrease of FRET$_E$ was fit to a single exponential with a time constant of τ = 1.2 min. Error bars represent the standard error of the mean.

(D) Schematic representation of the local positive feedback between HRas and PI3K in the nascent axonal growth cone.

(E) FRET$_E$ time-lapse analysis in Rat-2 fibroblasts transfected with CFP-HRas and YFP-RBD. EGF (50 ng/ml) leads to a marked HRas activation, which is strongly reduced upon LY294002 (50 μM) addition.

(F) HRas activation profile upon EGF and subsequent LY294002 addition.

(G) Chemical genetics approach to activate PI3K (see main text).

(H) Rat-2 fibroblasts expressing the indicated constructs were treated with iRap (5 μM) or EGF (10 ng/ml) and subjected to a Ras-GTP pull-down assay. Purified Ras-GTP and input material from the cell lysates were analyzed by western blotting. The western blots shown are representative of five independent experiments. Note that iRap addition leads to rapid increase in GTP-bound Ras.

(I) iRap-induced activation of Ras in live Rat-2 cells expressing LDR, CF-iSH, HRas, and YFP-RBD, as revealed by translocation of YFP-RBD to the plasma membrane.

near basal levels (Figures 2E and 2F), consistent with the presence of a positive feedback loop. In fibroblasts exhibiting high basal Ras activity, LY294002 addition also drastically reduced Ras activity (Figures S4C and S4D). We then took advantage of a chemical genetics strategy we recently developed to rapidly activate endogenous PI3K and asked whether activation of PI3K is sufficient to activate Ras. This approach is based on heterodimerization between a plasma-membrane-targeted form of FRB (Lyn_{11}-FRB, LDR) and a truncated form

of the PI3K regulatory subunit p85 flanked by CFP and FKBP (CF-iSH). This heterodimerization process, triggered by the small molecule iRap, results in translocation of the endogenous p110 catalytic subunit of PI3K to the plasma membrane and subsequent production of PIP3 [21] (Figure 2G). By using a Ras-GTP pull-down assay, we asked whether iRap-induced PI3K activation (monitored by akt phosphorylation) triggers Ras activation. Addition of iRap to fibroblasts cotransfected with LDR and CF-iSH led to a noticeable increase in phospho-Akt within 1 min (Figure 2H). In support of a positive feedback from PI3K to Ras, iRap-induced PI3K activation resulted in a significant increase of Ras-GTP within 1 min after stimulation (Figure 2H). As a control, Ras and PI3K activation were determined after EGF addition in mock-transfected cells (Figure 2H). As a second approach, we monitored the positive feedback from PI3K to Ras at the single-cell level. Fibroblasts were transfected with LDR and CF-iSH together with HRas and YFP-RBD. Addition of iRap led to translocation of CF-iSH (Figure 2I and Figure S5), activation of PI3K (Figure S5), and translocation of YFP-RBD to the plasma membrane (Figure 2I, Movie S2), indicating Ras activation. This further demonstrates the existence of a positive feedback from PI3K to Ras. The mechanism by which PI3K activates Ras is unknown. One possibility is that PI3K-induced PIP3 production regulates translocation of PH-domain containing Ras GEFs to the plasma membrane. Potential candidates include SOS and RasGRF, although clear evidence that PIP3 regulates these exchange factors is still lacking. It should be noted that we could not detect reliable PI3K activation in neurons by using this inducible system, perhaps because we found the LDR construct to be largely intracellular in these cells (data not shown). This prevented us from probing the PI3K-Ras feedback in neurons by using this approach.

Recruitment of HRas to the Axonal Growth Cone by Vesicular Transport

A plausible trigger for this local positive feedback loop in neurons is the recruitment of HRas to the nascent axon tip, which could then switch on the amplification circuit. This hypothesis was inspired by the observation of an increased concentration of HRas in the axonal growth cone (Figures S3A–S3C). A confocal ratio-imaging approach was used for quantification of the localization of CFP-HRas relative to that of YFP-KRas, which appears evenly distributed at the plasma membrane (Figures S3A and S3B). Although unpolarized cells exhibited fairly uniform distributions of CFP-HRas and YFP-KRas, polarized neurons showed a pronounced enrichment of CFP-HRas in the axon and a corresponding depletion of HRas in the remaining neurites relative to YFP-KRas (Figures 3A–3C). The polarized distribution of HRas was regulated by its C-terminal farnesyl-palmitoyl-targeting sequence because this motif, when fused to green fluorescent protein (GFP), was sufficient for axonal enrichment (data not shown). This is consistent with earlier work showing that a palmitoyl lipid modification is sufficient to target a peripheral membrane protein to the axon [22]. The absence of a palmitoyl modification in KRas, which is targeted to the plasma membrane by a farnesyl-polybasic motif instead [23], might explain why KRas is not enriched in the axon.

To address whether the polarized distribution of HRas results from vesicular transport of HRas to the axon tip, we made use of a photoactivatable (PA) GFP mutant [24] fused to HRas. After local photoconversion of PA-GFP-HRas in the soma (Figure 3D), individual vesicles were observed moving toward the tip of the axon (see Movie S3) with an average speed of $1.98 \pm 0.05\ \mu m/s$ (Figure 3E; see also Figure S6D), characteristic of fast axonal transport [25]. Vesicular transport of PA-GFP-KRas in the axon was not observed (Figures S6E and S6F and Movie S4). With the same photoactivation approach, the kinetics of Ras accumulation in axonal growth cones was measured in polarized neurons with an axon of $200 \pm 20\ \mu m$. PA-GFP-HRas appeared within minutes in vesicular structures and at the plasma membrane of the growth cone (Figures 3F–3H and Movie S5). In contrast, PA-GFP-KRas refilled the growth cone with much slower kinetics (Figures 3G and 3H; see also Figure S6G and Movie S6), consistent with passive diffusion along the plasma membrane. Thus, vesicular transport supplies HRas to the axon tip, explaining how local HRas concentration can rapidly increase during axon formation. This suggests that the HRas-PI3K feedback loop is locally reinforced by HRas recruitment, thereby providing a trigger mechanism that initiates axon formation. Because accumulation of HRas to the axon tip is mediated, at least in part, by its palmitoyl modification, it is likely that other palmitoylated Ras isoforms, i.e., NRas and RRas, will be transported to the axon tip and will contribute to this local feedback loop. Local accumulation in the nascent axon and a role in axon specification have previously been described for RRas [14]. Finally, because bulk membrane trafficking is directed to the growing axon [26–28], it is reasonable to assume that HRas is only one out of several components of this feedback circuit to be transported to the nascent axon.

Competitive Neurite Outgrowth

Although reinforced local positive feedback provides a powerful amplification mechanism to form an axon, a second mechanism is needed to ensure that this positive feedback is only triggered in one of the neurites. Because HRas is recruited to the nascent axon, a plausible mechanism for the prevention of multiaxon formation is that individual neurites compete for a limiting pool of HRas. This competition model stipulates that recruitment of HRas to the nascent axon leads to simultaneous depletion of HRas in the other neurites. This would guarantee that the local HRas-PI3K feedback is reinforced in the future axon and concomitantly weakened in the other neurites. Consistent with the presence of a limiting pool of HRas, we found that accumulation of HRas in the axon leads to reduced HRas concentration in the other neurites (Figures 3A–3C).

This competition model further predicts that extension of the nascent axon is coupled to inhibition of growth in the remaining neurites. We monitored changes in the surface area of the future axon versus the remaining neurites during neuronal polarization and found that reversible membrane extensions in the future axon are often accompanied by rapid retractions in the other neurites. Coupling between extension and retraction events was

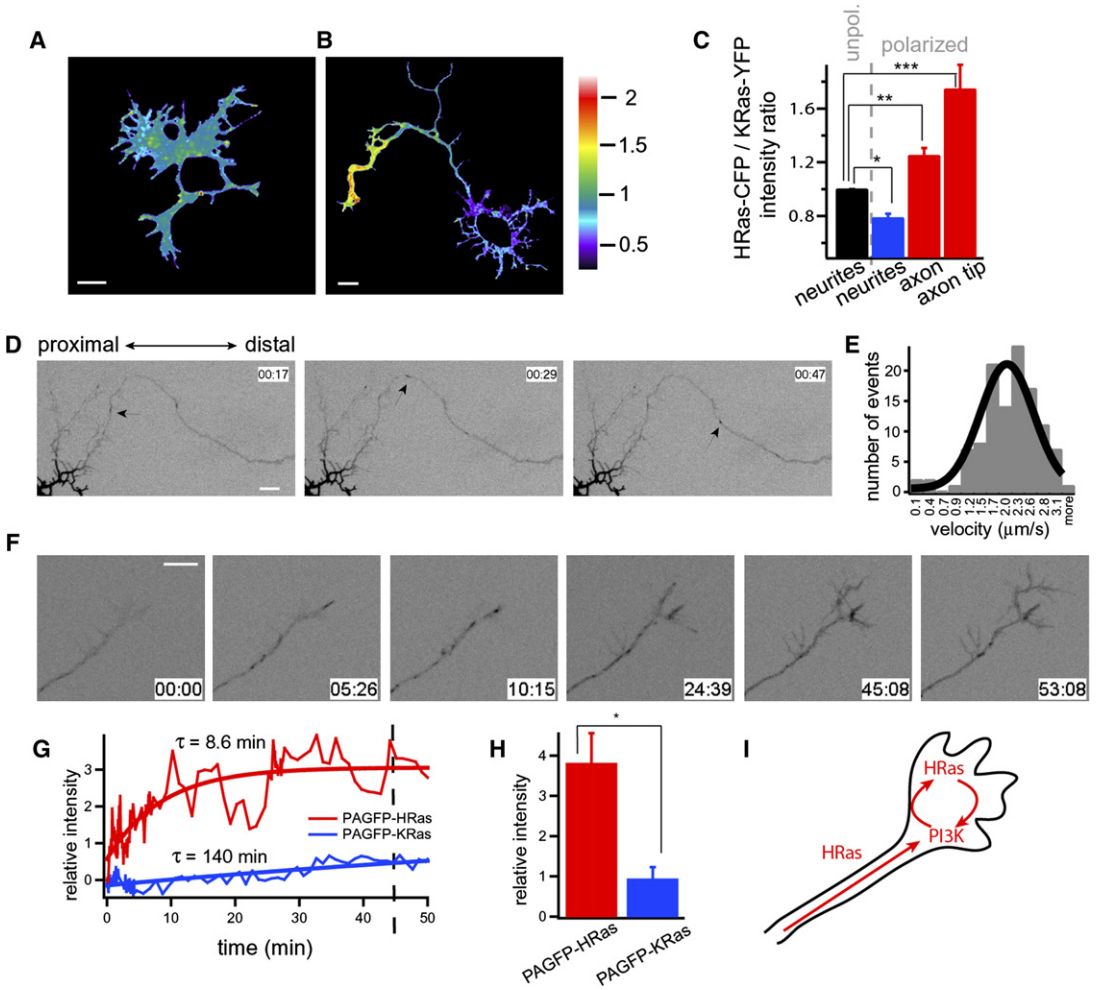

Figure 3. HRas Is Recruited in the Axonal Growth Cone

(A–C) CFP-HRas over YFP-KRas ratio imaging in unpolarized (DIV 1) and polarized (DIV 3) neurons. YFP-KRas was used as a uniform plasma membrane reference. The relative HRas concentration was fairly uniform before axon formation (n = 12 [A and C]) but increased in newly formed axons with a corresponding decrease in the remaining neurites (n = 12 [B and C]). * indicates p = 2.5×10^{-5}, ** indicates p = 0.0003, and *** indicates p = 0.0008).

(D) Time-lapse analysis of PA-GFP-HRas-containing vesicles moving toward the axon tip after photoconversion in the soma (see Figures S6A–S6C for a full view of the cell). The arrow points to a single moving vesicle. Time is in seconds (see Movie S3).

(E) Velocity distribution of PA-GFP-HRas vesicles moving toward the axon tip.

(F) Time-lapse analysis of PA-GFP-HRas accumulation in the axonal growth cone after photoactivation in the soma. The axon is about 200 μm long. Time is in minutes (see Movie S5).

(G) Kinetics of transport-mediated PA-GFP-HRas accumulation in the axonal growth cone. Photoactivated PA-GFP-KRas reached the growth cone with much slower kinetics (see also Movie S6 and Figure S6G).

(H) Comparison of GFP fluorescence intensities in axonal growth cones measured 45 min after photoconversion of PA-GFP HRas (n = 6) or PA-GFP-KRas (n = 5) in the soma (* indicates p = 0.0008), in neurons that have an axon of 200 (± 20) μm.

(I) Schematic representation of HRas vesicular transport as a mechanism to reinforce the local HRas-PI3K feedback loop.

Error bars represent the standard error of the mean.

particularly obvious during axon specification, when the burst of axon growth was consistently associated with a significant retraction of the remaining neurites (Figure 4A and Figure S7; see also Movie S7). To quantify the negative coupling between axon and neurite extensions, we measured the crosscorrelation between changes in axonal versus nonaxonal surface areas in eight neurons undergoing polarization. The mean crosscorrelation function shows a distinct negative peak, confirming the competing nature of axon and neurite extensions (Figure 4B). This rapid coupling between axon extension and neurite retraction is consistent with a depletion process by which HRas and possibly other components are selectively recruited to the winning axon and reduced in the remaining neurites.

Robust Symmetry Breaking and Single-Axon Formation by Reinforced Positive Feedback

We used mathematical modeling to assess whether a local HRas-PI3K positive feedback loop coupled to polarized transport of a limited pool of HRas is sufficient to guarantee the formation of a single axon. Computer simulations of neuronal polarization based on this molecular circuit led to robust formation of a single axon and recapitulated the competing nature of neurite outgrowth (Figures 4C–4E and Movie S8; see

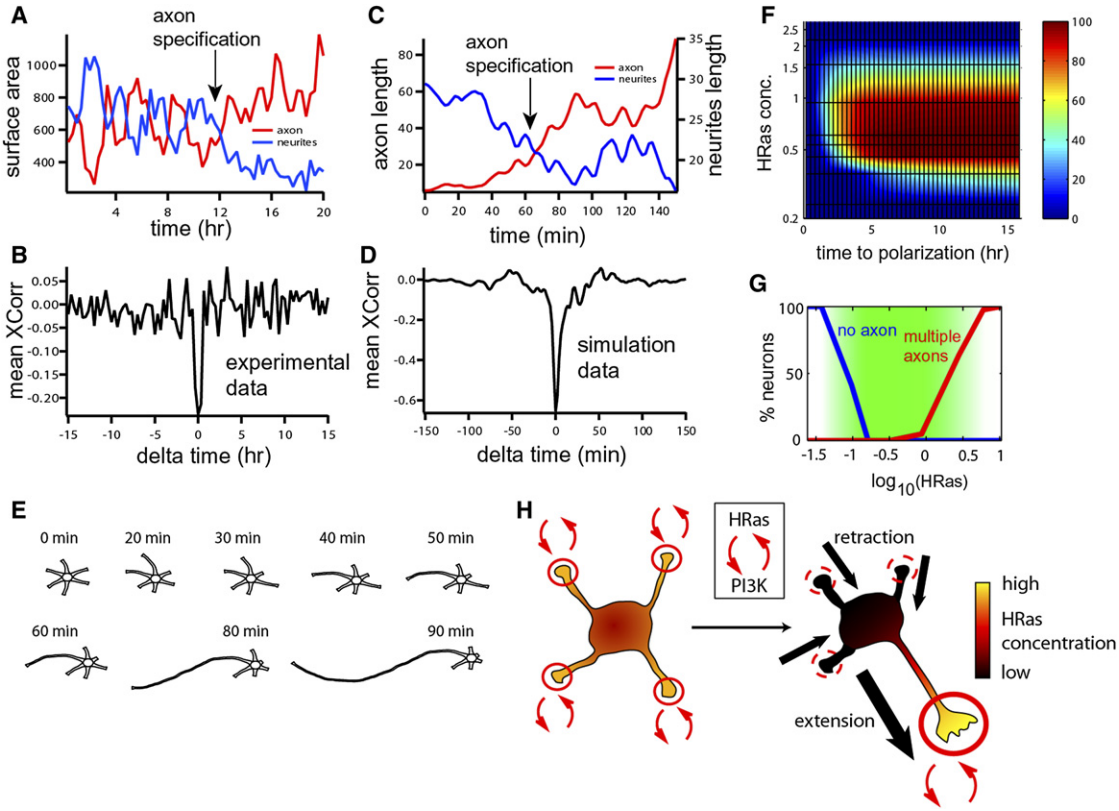

Figure 4. Positive Feedback Coupled to Recruitment Is a Robust Signaling Circuit for Symmetry Breaking

(A and B) Correlation between extension of the future axon and retraction of other neurites during neuronal polarization. (A) shows a plot of changes in the surface areas of the future axon (red) and remaining neurites (blue) as a function of time (see Figure S7 and Movie S7 for image data). (B) presents crosscorrelation analysis showing that changes in axonal and nonaxonal neurite areas are negatively correlated (n = 8 cells). (C–G) Computer simulations of neuronal polarization based on the signaling circuit described in the text. (C) and (D) show simulations that recapitulate the correlation between the extension of the nascent axon and retraction of other neurites. (C) shows analysis of axon and neurites length in one simulation run. (D) shows mean crosscorrelation analysis for changes in axonal versus neurites length (n = 16 simulations). (E) show snapshots of a typical simulation run (see Movie S8). (F) presents a surface plot showing the percent of neurons (displayed in a color-coded scale) developing a single axon as a function of HRas concentration and time. (G) shows the percent of neurons with no or multiple axons as a function of HRas concentration. The green area indicates the HRas concentration range over which neurons have a high probability to form a single axon. (H) Model for symmetry breaking and single-axon formation.

Supplemental Data for a formal description of the mathematical model). Symmetry breaking and single-axon formation were observed over a wide range of initial HRas concentrations (Figure 4F). However, no axon or multiple axons formed for HRas concentrations either below or above the optimal concentration window (Figure 4G and Figure S8), consistent with the phenotypes we observed upon HRas knockdown or overexpression (Figures 1A–1C).

In conclusion, our work provides evidence for the existence of a feedback loop between HRas and PI3K locally reinforced by HRas transport from a limiting cellular pool. The spatial and temporal dynamics of this signaling circuit are consistent with a role in neuronal symmetry breaking and single-axon formation (Figure 4H). It is in this context interesting to note that mice lacking both HRas and NRas are viable and don't have an obvious neuronal development phenotype [29]. This could be due to Ras isoform redundancy or other compensatory mechanisms. It is likely that other Ras isoforms enriched in the nascent axon tip contribute to this feedback loop, such as RRas, which has been recently identified as another regulator of axon specification [14]. Our mathematical model predicts that local positive feedback coupled to vesicular transport guarantees the formation of an axon in the absence of extrinsic spatial cues and explains how a single axon emerges from competing neurites. In an in vivo setting where newly formed axons are in many cases spatially oriented [30], extrinsic cues might locally enhance the HRas-PI3K feedback circuit and spatially bias neuronal polarization. The robustness of this simple feedback circuit makes it likely that positive feedback coupled to recruitment of a limited pool of an activator is a general mechanism for cell symmetry breaking.

Supplemental Data

Experimental Procedures, eight figures, and eight movies are available at http://www.current-biology.com/cgi/content/full/18/1/44/DC1/.

Acknowledgments

We thank Dan Kaplan, Namiko Abe, Lubert Stryer, James Ferrell, Craig Garner, Rich Reimer, Angie Hahn, Phil Vitorino, Annette Salmeen, and Onn Brandmann for critical reading of the manuscript and insightful comments. We also thank Emmanuel Guignet for his

help with electroporation experiments. This work is supported by the National Institutes of Health grant MH64801 to T.M.

Received: May 3, 2007
Revised: November 17, 2007
Accepted: November 19, 2007
Published online: December 27, 2007

References

1. Dotti, C.G., Sullivan, C.A., and Banker, G.A. (1988). The establishment of polarity by hippocampal neurons in culture. J. Neurosci. *8*, 1454–1468.
2. Shi, S.H., Cheng, T., Jan, L.Y., and Jan, Y.N. (2004). APC and GSK-3beta are involved in mPar3 targeting to the nascent axon and establishment of neuronal polarity. Curr. Biol. *14*, 2025–2032.
3. Inagaki, N., Chihara, K., Arimura, N., Menager, C., Kawano, Y., Matsuo, N., Nishimura, T., Amano, M., and Kaibuchi, K. (2001). CRMP-2 induces axons in cultured hippocampal neurons. Nat. Neurosci. *4*, 781–782.
4. Shi, S.H., Jan, L.Y., and Jan, Y.N. (2003). Hippocampal neuronal polarity specified by spatially localized mPar3/mPar6 and PI 3-kinase activity. Cell *112*, 63–75.
5. Zhou, F.Q., Zhou, J., Dedhar, S., Wu, Y.H., and Snider, W.D. (2004). NGF-induced axon growth is mediated by localized inactivation of GSK-3beta and functions of the microtubule plus end binding protein APC. Neuron *42*, 897–912.
6. Schwamborn, J.C., and Puschel, A.W. (2004). The sequential activity of the GTPases Rap1B and Cdc42 determines neuronal polarity. Nat. Neurosci. *7*, 923–929.
7. Yoshimura, T., Kawano, Y., Arimura, N., Kawabata, S., Kikuchi, A., and Kaibuchi, K. (2005). GSK-3beta regulates phosphorylation of CRMP-2 and neuronal polarity. Cell *120*, 137–149.
8. Jiang, H., Guo, W., Liang, X., and Rao, Y. (2005). Both the establishment and the maintenance of neuronal polarity require active mechanisms: Critical roles of GSK-3beta and its upstream regulators. Cell *120*, 123–135.
9. Yoshimura, T., Arimura, N., Kawano, Y., Kawabata, S., Wang, S., and Kaibuchi, K. (2006). Ras regulates neuronal polarity via the PI3-kinase/Akt/GSK-3beta/CRMP-2 pathway. Biochem. Biophys. Res. Commun. *340*, 62–68.
10. Kim, W.Y., Zhou, F.Q., Zhou, J., Yokota, Y., Wang, Y.M., Yoshimura, T., Kaibuchi, K., Woodgett, J.R., Anton, E.S., and Snider, W.D. (2006). Essential roles for GSK-3s and GSK-3-primed substrates in neurotrophin-induced and hippocampal axon growth. Neuron *52*, 981–996.
11. Bradke, F., and Dotti, C.G. (1999). The role of local actin instability in axon formation. Science *283*, 1931–1934.
12. Baas, P.W. (1997). Microtubules and axonal growth. Curr. Opin. Cell Biol. *9*, 29–36.
13. Rodriguez-Viciana, P., Warne, P.H., Dhand, R., Vanhaesebroeck, B., Gout, I., Fry, M.J., Waterfield, M.D., and Downward, J. (1994). Phosphatidylinositol-3-OH kinase as a direct target of Ras. Nature *370*, 527–532.
14. Oinuma, I., Katoh, H., and Negishi, M. (2007). R-Ras controls axon specification upstream of glycogen synthase kinase-3beta through integrin-linked kinase. J. Biol. Chem. *282*, 303–318.
15. Bivona, T.G., Perez De Castro, I., Ahearn, I.M., Grana, T.M., Chiu, V.K., Lockyer, P.J., Cullen, P.J., Pellicer, A., Cox, A.D., and Philips, M.R. (2003). Phospholipase Cgamma activates Ras on the Golgi apparatus by means of RasGRP1. Nature *424*, 694–698.
16. Zal, T., and Gascoigne, N.R. (2004). Photobleaching-corrected FRET efficiency imaging of live cells. Biophys. J. *86*, 3923–3939.
17. Liou, J., Fivaz, M., Inoue, T., and Meyer, T. (2007). Live-cell imaging reveals sequential oligomerization and local plasma membrane targeting of STIM1 following Ca2+ store depletion. Proc. Natl. Acad. Sci. USA *104*, 9301–9306.
18. Kontos, C.D., Stauffer, T.P., Yang, W.P., York, J.D., Huang, L., Blanar, M.A., Meyer, T., and Peters, K.G. (1998). Tyrosine 1101 of Tie2 is the major site of association of p85 and is required for activation of phosphatidylinositol 3-kinase and Akt. Mol. Cell. Biol. *18*, 4131–4140.
19. Sasaki, A.T., Chun, C., Takeda, K., and Firtel, R.A. (2004). Localized Ras signaling at the leading edge regulates PI3K, cell polarity, and directional cell movement. J. Cell Biol. *167*, 505–518.
20. Sasaki, A.T., Janetopoulos, C., Lee, S., Charest, P.G., Takeda, K., Sundheimer, L.W., Meili, R., Devreotes, P.N., and Firtel, R.A. (2007). G protein-independent Ras/PI3K/F-actin circuit regulates basic cell motility. J. Cell Biol. *178*, 185–191.
21. Suh, B.C., Inoue, T., Meyer, T., and Hille, B. (2006). Rapid chemically induced changes of PtdIns(4,5)P2 gate KCNQ ion channels. Science *314*, 1454–1457.
22. El-Husseini, Ael-D., Craven, S.E., Brock, S.C., and Bredt, D.S. (2001). Polarized targeting of peripheral membrane proteins in neurons. J. Biol. Chem. *276*, 44984–44992.
23. Hancock, J.F. (2003). Ras proteins: Different signals from different locations. Nat. Rev. Mol. Cell Biol. *4*, 373–384.
24. Patterson, G.H., and Lippincott-Schwartz, J. (2002). A photoactivatable GFP for selective photolabeling of proteins and cells. Science *297*, 1873–1877.
25. Brady, S.T. (1991). Molecular motors in the nervous system. Neuron *7*, 521–533.
26. Bradke, F., and Dotti, C.G. (1997). Neuronal polarity: Vectorial cytoplasmic flow precedes axon formation. Neuron *19*, 1175–1186.
27. de Anda, F.C., Pollarolo, G., Da Silva, J.S., Camoletto, P.G., Feiguin, F., and Dotti, C.G. (2005). Centrosome localization determines neuronal polarity. Nature *436*, 704–708.
28. Gartner, A., Huang, X., and Hall, A. (2006). Neuronal polarity is regulated by glycogen synthase kinase-3 (GSK-3beta) independently of Akt/PKB serine phosphorylation. J. Cell Sci. *119*, 3927–3934.
29. Esteban, L.M., Vicario-Abejon, C., Fernandez-Salguero, P., Fernandez-Medarde, A., Swaminathan, N., Yienger, K., Lopez, E., Malumbres, M., McKay, R., Ward, J.M., et al. (2001). Targeted genomic disruption of H-ras and N-ras, individually or in combination, reveals the dispensability of both loci for mouse growth and development. Mol. Cell. Biol. *21*, 1444–1452.
30. Adler, C.E., Fetter, R.D., and Bargmann, C.I. (2006). UNC-6/Netrin induces neuronal asymmetry and defines the site of axon formation. Nat. Neurosci. *9*, 511–518.